

**Studies in Surface Science and Catalysis**

Advisory Editors: B. Delmon and J.T. Yates

Vol. 84

# **ZEOLITES AND RELATED MICROPOROUS MATERIALS: STATE OF THE ART 1994 PART C**

**Proceedings of the 10th International Zeolite Conference,  
Garmisch-Partenkirchen, Germany, July 17–22, 1994**

Editors

**J. Weitkamp**

*University of Stuttgart, Stuttgart, Germany*

**H.G. Karge**

*Fritz Haber Institute of the Max Planck Society, Berlin, Germany*

**H. Pfeifer**

*University of Leipzig, Leipzig, Germany*

**W. Hölderich**

*University of Technology (RWTH), Aachen, Germany*



**ELSEVIER**

**Amsterdam — London — New York — Tokyo**

**1994**

## CONTENTS

### Part A.

Preface (by the Editors)	xxxix
Acknowledgments (by the Editors)	xxxiii
Committees	xxxiv
International Advisory Board	xxxv
Financial Support	xxxvii

### I. Synthesis

<b>PL01</b>	<b>Zeolites and their Mechanism of Synthesis</b>	
	<i>E. J. P. Feijen, J. A. Martens, P. A. Jacobs</i>	3
A001	The Role of Diquaternary Cations as Directing Agents in Zeolite Synthesis	
	<i>A. Moini, K.D. Schmitt, E.W. Valyocsik and R.F. Polomski</i>	23
A002	A Study of Guest/Host Energetics for the Synthesis of Cage Structures NON and CHA	
	<i>T.V. Harris and S.I. Zones</i>	29
A003	Zeolite MCM-22: Synthesis, Dealumination and Structural Characterization	
	<i>S. Unverricht, M. Hunger, S. Ernst, H.G. Karge and J. Weitkamp</i>	37
A004	Molecular Sieves from Pillaring of Layered Silicates	
	<i>S.-T. Wong, S.-H. Wong, S.-B. Liu and S. Cheng</i>	45
A010	Development of a formation mechanism for M41S materials	
	<i>J.C. Vartuli, K.D. Schmitt, C.T. Kresge, W.J. Roth, M.E. Leonowicz, S.B. McCullen, S.D. Hellring, J.S. Beck, J.L. Schlenker, D. H. Olson and E. W. Sheppard</i>	53
A011	Synthesis of Al-Containing MCM-41 Materials: Template Interaction and Removal	
	<i>R. Schmidt, D. Akporiaye, M. Stöcker and O.H. Ellestad</i>	61
A012	Preparation and Properties of Ti-Containing MCM-41	
	<i>A. Corma, M.T. Navarro, J. Pérez-Pariente and F. Sánchez</i>	69

The figures before the articles indicate the paper numbers used during the Conference
---

A013	New Mesoporous Titanosilicate Molecular Sieve <i>O. Franke, J. Rathousky, G. Schulz-Ekloff, J. Stárek and A. Zukal</i>	77
A014	Amorphous Mesoporous Silica-Alumina with Controlled Pore Size as Acid Catalyst <i>G. Bellussi, C. Perego, A. Carati, S. Peratello, E. Previde Massara and G. Perego</i>	85
A024	Nonaqueous Synthesis of Large Zeolite and Molecular Sieve Crystals <i>S. Nadimi, S. Oliver, A. Kuperman, A. Lough, G.A. Ozin, J.M. Garcés, M.M. Olken and P. Rudolph</i>	93
A025	Diversity of the System $\text{Ga}_2\text{O}_3\text{-P}_2\text{O}_5\text{-H}_2\text{O-HF}$ in the Presence of Organic Species <i>C. Schott-Darje, H. Kessler, M. Soulard, V. Gramlich and E. Benazzi</i>	101
A027	Convenient Synthesis of Crystalline Microporous Transition Metal Silicates Using Complexing Agents <i>R. Kumar, A. Raj, S.B. Kumar and P. Ratnasamy</i>	109
A028	Occurrence of Differently Coordinated Framework Heteroatoms within One Zeolite Sample: The Example of MFI Type Vanadium Silicalite, KVS-5 <i>J. Kornatowski, B. Wichterlová, M. Rozwadowski and W.H. Baur</i>	117
A029	Synthesis and Characterization of Highly Ordered Mesoporous Material FSM-16, from a Layered Polysilicate <i>S. Inagaki, Y. Fukushima and K. Kuroda</i>	125
P001	Zeolite Synthesis Using Catalytic Amounts of Template: Structure Blocking Effects and Stoichiometric Syntheses <i>J.L. Casci</i>	133
P002	Simultaneous Occurrence of Differently Coordinated Framework Heteroatoms in One Zeolite: MFI Type Vanadium Silicalite, KVS-5 <i>G. Giordano, F. Di Renzo, F. Remoué, F. Fajula, D. Plee and P. Schulz</i>	141
P003	Nucleation Gels for the Synthesis of Faujasite Type Zeolites <i>H. Lechert, P. Staelin and M. Wrobel and U. Schimmel</i>	147
P004	Synthesis of Omega Zeolite without Use of Tetramethylammonium (TMA) Ions <i>S. Yang and N.P. Evmiridis</i>	155
P005	Synthesis of Aluminium-Rich Zeolite Beta <i>F. Vaudry, F. Di Renzo, F. Fajula and P. Schulz</i>	163

- P006 The Influence of Alkali Cation on the Synthesis of Zeolite Beta from Fluoride Containing Gels  
*R. Mostowicz, F. Testa, F. Crea, A. Nastro, R. Aiello, A. Fonseca and J.B. Nagy* 171
- P007 In situ studies of zeolite syntheses using powder diffraction methods. Crystallization of "instant zeolite A" powder and synthesis of CoAPO-5  
*P. Norby, A.N. Christensen and J.C. Hanson* 179
- P008 In-Situ Observation of Crystal Growth of Silicalite under Hydrothermal Synthesis Condition  
*T. Sano, S. Sugawara, Y. Kawakami, A. Iwasaki, M. Hirata, I. Kudo, M. Ito and M. Watanabe* 187
- P009 Zeolite ZSM-5 Synthesized in the Extremely Dense System  
*Li Jianquan, Liu Guanghuan, Dong Jinxiang, Do Tao and Tomoyuki Inui* 195
- P010 Ammonium-Based Alkaline-Free Synthesis of MFI-Type Boron- and Titanium-Zeolites  
*U. Müller and W. Steck* 203
- P011 On the Synthesis and Characterization of Cr-Silicalite-1  
*N. van der Puil, Widyawati, J.C. Jansen and H. van Bekkum* 211
- P012 New Insights into the Mode of Formation of AlPO<sub>4-n</sub> Molecular Sieves  
*S. Oliver, A. Kuperman, A. Lough, G.A. Ozin, J.M. Garcés, M.M. Olken and P. Rudolph* 219
- P013 Synthesis and Characterization of SnAPO-5  
*K. Vinje and K.P. Lillerud* 227
- P014 Reverse Micelle Based Synthesis of Microporous Materials in Hydrocarbon Solvents  
*P.K. Dutta, M. Jacupca, L. Savati, K.S.N. Reddy and R.R. Ansari* 235
- P015 Aluminum Incorporation in Mesoporous Molecular Sieves  
*M. Janicke, D. Kumar, G.D. Stucky and B.F. Chmelka* 243
- P016 A Novel Lead Titanate Microporous Crystal with Nanometer Size  
*Y. Guo, S. Qiu, W. Pang, N. Ohnishi and K. Hiraga* 251
- P017 Electron Diffraction and Infrared Spectroscopy of Amorphous Aluminosilicate Gels  
*B. Subotic, A.M. Tonejc, D. Bagovic, A. Cizmek and T. Antonic* 259

P018	Some Aspects of the Preparation and Catalytic Activity of Chromia Pillared Montmorillonite <i>M. Sychev, V.H.J. de Beer, R.A. van Santen, R. Prihod'ko and V. Goncharuk</i>	267
P019	Aluminium-Free Layer Silicates as a Basic System for the Preparation of Pillared Clays <i>W. Schwieger, K. Pohl, U. Brenn and H.G. Karge</i>	275
P020	Synthesis and MAS-NMR Analysis of Highly Stable Pillared Clays <i>J. Espinosa, S. Gómez and G.A. Fuentes</i>	283
P021	Influence of Crystalline Seeds on the Zeolitization of Volcanic Ashes: A Calorimetric Study <i>G.N. Kirov and N. Petrova</i>	291
P022	The Formation of Analcime from Laumontite in the Smrekovec Volcanics, NW Slovenia - An Experimental Approach <i>U. Barth-Wirsching, D. Klammer and P. Kovic-Kralj</i>	299
C020	Oriented Coatings of Silicalite-1 for Gas Sensor Applications <i>J.H. Koegler, H.W. Zandbergen, J.L.N. Harteveld, M.S. Nieuwenhuizen, J.C. Jansen and H. van Bekkum</i>	307
C021	Synthesis and Characterization of a Novel Microporous Boron-Aluminum Chloride with a Cationic Framework <i>J. Yu, K. Tu and R. Xu</i>	315
C022	Use of Diels-Alder Derived Templates to Prepare Zeolites with Multidimensional Pore Systems <i>Y. Nakagawa</i>	323
C023	Synthesis, Characterization and Catalytic Properties of Zeolite PSH-3/MCM-22 <i>R. Ravishankar, Tapas Sen, V. Ramaswamy, H.S. Sony, S. Ganapathy and S. Sivasanker</i>	331

## II. Structure and Characterization

<b>PL02</b>	<b>Advances in Powder Diffraction Methods for Zeolite Structure Analysis</b> <i>L. B. McCusker</i>	341
B001	Low-Temperature <sup>1</sup> H MAS NMR Investigations on the Nature of Acid Sites Causing Enhanced Catalytic Activity in H-Zeolites <i>E. Brunner, K. Beck, M. Koch, H. Pfeifer, B. Staudte and D. Zscherpel</i>	357

- B002 Brønsted Acidity in US-Y Zeolites  
*M.A. Makarova, A. Garforth, V.L. Zhobolenko, J. Dwyer, G.J. Earl and D. Rawlence* 365
- B003 Acidic Properties of Metal Substituted Aluminophosphates Studied by Adsorption Calorimetry and IR Spectroscopy  
*J. Jänchen, M.J. Haanepen, M.P.J. Peeters, J.H.M.C. van Wolput, J.P. Wolthuizen and J.H.C. van Hooff* 373
- B004 Multinuclear NMR Studies of Acid Sites in Zeolites  
*H. Ernst, D. Freude, H. Pfeifer and I. Wolf* 381
- B010 Tracing the Production of Spinel Based Ceramics from the Heat Induced Transformations of Zinc and Cobalt Exchanged Zeolite-A Using Combined XRD/XAFS Techniques  
*L.M. Colyer, G. N. Greaves, A.J. Dent, S.W. Carr, K.K. Fox and R.H. Jones* 387
- B011 Synthesis and Characterization by X-Ray diffraction and solid state NMR of ULM-5, a new fluorinated gallophosphate  $\text{Ga}_{16}(\text{PO}_4)_{14}(\text{HPO}_4)_2(\text{OH})_2\text{F}_7$ ,  $4 \text{H}_3\text{N}(\text{CH}_2)_6\text{NH}_3$ ,  $6\text{H}_2\text{O}$  with 16-membered rings  
*T. Loiseau, D. Riou, F. Taulelle and G. Férey* 395
- B012 Framework Fe Sites in Sodalite: A Model for Fe T Sites in Zeolites  
*D. Goldfarb, M. Bernardo, K.G. Strohmaier, D.E.W. Vaughan and H. Thomann* 403
- B013 Microporous Titanosilicate ETS-10: Electron Microscopy Study  
*T. Ohsuna, O. Terasaki, D. Watanabe, M.W. Anderson and S. Lidin* 413
- B014 Exploring Cation Siting in Zeolites by Solid-State NMR of Quadrupolar Nuclei  
*G. Engelhardt, M. Hunger, H. Koller and J. Weitkamp* 421
- B018 An In-Situ X-Ray and NMR Study of the Formation of Layered Silicate Mesophase Materials  
*L.M. Bull, D. Kumar, S.P. Millar, T. Besier, M. Janicke, G.D. Stucky and B.F. Chmelka* 429
- B019 RUB-10, a Boron Containing Analogue of Zeolite NU-1  
*U. Oberhagemann, B. Marler, I. Topalovic and H. Gies* 435
- B020 Structural Analysis by Neutron Diffraction of Simple Gases ( $\text{H}_2$ , Ar,  $\text{CH}_4$  and  $\text{CF}_4$ ) Sorbed Phases on  $\text{AlPO}_4$ -5  
*J.P. Coulomb, C. Martin, Y. Grillet and N. Tosi-Pelleng* 445

B022	Temperature Program Desorption and Reduction Studies of Octahedral Molecular Sieves <i>Y.-G. Yin, W.-Q. Xu, R. DeGuzman, Y. F. Shen, S.L. Suib and C.-L. O'Young</i>	453
A026	Effect of the stacking probability on the properties of the molecular sieves CIT-1, SSZ-26 and SSZ-33 <i>R.F. Lobo, S.I. Zones and M.E. Davis</i>	461
B030	Muon Spin Relaxation Studies of Cyclohexadienyl Radicals in NaUSY <i>M. Shelley, D.J. Arseneau, M. Senba, J.J. Pan, R. Snooks, S. R. Kreitzman and D.G. Fleming</i>	469
B031	Factors affecting the UV-Transparency of Molecular Sieves <i>S. Engel, U. Kynast, K. K. Unger and F. Schüth</i>	477
B032	The Study of the Surface Topography of Microporous Materials Using Atomic Force Microscopy <i>M.L. Occelli, S.A.C. Gould and G.D. Stucky</i>	485
B033	Time Dependence of Vibrational Relaxation of Deuterated Hydroxyls in Acidic Zeolites <i>M. Bonn, M.J.P. Brugmans, A.W. Kleyn, R.A. van Santen and A. Legendijk</i>	493
B034	Characterization of Titanium Silicalites Using Cyclic Voltammetry <i>S. de Castro-Martins, A. Tuel and Y. Ben Taarit</i>	501
B035	Copper Exchanged Zeolites Studied with $^{13}\text{C}$ and $^{129}\text{Xe}$ NMR of Adsorbed Carbon Monoxide and Xenon <i>M. Hartmann and B. Boddenberg</i>	509
B036	Two-Dimensional $^{129}\text{Xe}$ Exchange NMR Measurements of Xenon Dynamics in Na-A Zeolite <i>M. Janicke, B.F. Chmelka, R.G. Larsen, J. Shore, K. Schmidt-Rohr, L. Emsley, H. Long and A. Pines</i>	519
B037	Electron Transfer Reactions in H-Mordenite <i>R. Crockett and E. Roduner</i>	527
P041	Faults, Intergrowths, and Random Phases in the ABC-D6R Family of Zeolites <i>R. Szostak and K.P. Lillerud</i>	535
P042	Systematic Relationships between the Structures of CHA, AEI and KFI <i>K.P. Lillerud and D. Akporiaye</i>	543

P043	The Essential Identity of the Framework Structures of ZSM-8 and ZSM-5 <i>C. Weidenthaler, R.X. Fischer and R.D. Shannon</i>	551
P044	Orthorhombic and Monoclinic Silicalites: Structure, Morphology, Vibrational Properties and Crystal Defects <i>G.L. Marra, G. Tozzola, G. Leofanti, M. Padovan, G. Petrini, F. Genoni, B. Venturelli, A. Zecchina, S. Bordiga and G. Ricciardi</i>	559
P045	Deformation Analysis of the D8R-Unit in Zeolite Structures <i>A. Bieniok and H.-B. Bürgi</i>	567
P046	Systematic Evaluation and Classification of Zeolite Frameworks Based on Constituent Sheets <i>D.E. Akporiaye</i>	575
P047	Generation of 4-Connected 3-Dimensional Nets Using Complex Nodes <i>K. Reinecke</i>	583
P048	Si, Al Distribution in Zeolite Frameworks with Special Reference to Dempsey's Rule <i>M. Sato, K. Maeda and K. Hirasawa</i>	589
P049	Crystalline Galliosilicates with the Natrolite Structure <i>M.L. Occelli, E. Goldish and H. Eckert</i>	597
P050	Synthesis and Characterization of an Aluminophosphate Material with AIPO-15 Framework Type Structure <i>N. Bilba, A. Azzouz, N. Naum and D. Nibou</i>	605
P051	Modifications of Structure and Si Environment Upon Heating of SAPO-5, SAPO-34 and SAPO-37 <i>M. Briend, M.J. Peltre, P. Massiani, P.P. Man, R. Vomscheid, M. Derewinski and D. Barthomeuf</i>	613
P052	The Structure of a Krypton Encapsulate of Zeolite A <i>N.H. Heo, K.H. Cho, and K. Seff</i>	621
P053	The Structure of the Tetrahedral $\text{Na}_5^{4+}$ Cluster in Zeolite X <i>Y. Kim, Y.W. Han and K. Seff</i>	629
P054	Structural Modifications Induced by Dehydration in Yugawaralite <i>A. Alberti, S. Quartieri and G. Vezzalini</i>	637
P055	Thermal Behavior of Heulandites and Clinoptilolites of Western Anatolia <i>F. Esenli and I. Kumbasar</i>	645
P056	Acidic Properties of Titanium-Silicalites-1 <i>A. Auroux, A. Gervasini, E. Jorda and A. Tuel</i>	653



P057	Probing Acid Sites in Zeolites by X-Ray Photoelectron Spectroscopy using Pyridine as a Probe Molecule <i>R.B. Borade and A. Clearfield</i>	661
P058	Temperature-Programmed Desorption (TPD) of N-Methyl-Pyrrolidine on HNaY Zeolites <i>B. Hunger and M.v. Szombathely</i>	669
P059	High Temperature Calorimetry of MCM-41 <i>I. Petrovic, A. Navrotsky, C.-Y. Chen and M.E. Davis</i>	677
P060	A Comparative Study of the Acidity of Various Zeolites Using the Differential Heats of Ammonia Adsorption as Measured by High-Vacuum Microcalorimetry <i>H.G. Karge and L.C. Jozefowicz</i>	685
P061	Microcalorimetric Studies of the Acidity of Several Zeolites with the Offretite-Erionite Structure <i>A. Auroux and M.L. Occelli</i>	693
P062	Quantification of Acidity in H-ZSM-5 <i>D.J. Parrillo, A. Biaglow, R.J. Gorte and D. White</i>	701
P063	Variable-Temperature <sup>1</sup> H MAS NMR Investigations on the Interaction between Brønsted Acid Sites and Carbon Monoxide Adsorbed on H-ZSM-5 Zeolites <i>M. Koch, E. Brunner, D. Fenzke, H. Pfeifer and B. Staudte</i>	709
P064	Application of Iodometry for Zeolite Active Sites Characterization and Modification <i>I.I. Ivanova, A.D. Kazenina, B.V. Romanovsky and I. M. Gerzeliev</i>	717
P066	Cation Migration in Zeolite LaNaY Investigated by Multi-Nuclear Solid-State NMR <i>M. Hunger, G. Engelhardt and J. Weitkamp</i>	725
P067	<sup>6</sup> Li NMR Studies of Zeolite Li <sub>4</sub> NagA <i>B. Schimiczek, R. Greth and B. Boddenberg</i>	733
P068	Cation Segregation in Simulated Radioactive-Waste Zeolite-A Mixtures <i>J.W. Richardson, Jr., M. A. Lewis and B.R. McCart</i>	741
P069	The Effect of Precursor Forms on the Dispersion and Related Properties of Ruthenium in Y Zeolite <i>L.-H. Lin and K.-J. Chao</i>	749

- P070 Characterization and Catalytic Properties of Zeolite-Supported Platinum-Iridium Bimetallic Catalysts Prepared by Decoration of Platinum with Iridium  
*I.C. Hwang and S.I. Woo* 757
- P071 Clustering of Platinum Atoms in Zeolite EMT Supercage: Comprehensive Physicochemical Characterization  
*H. Ihee, T. Becue, R. Ryoo, C. Potvin, J.-M. Manoli and G. Djéga-Mariadassou* 765
- P072 XAS Studies on the Interaction of Chlorobenzene with PtY and PdY Zeolites  
*U. Hatje, M. Hagelstein and H. Förster* 773
- P073 Deuterium of Methane as a Test Reaction on Pt Dispersion in Mazzite Zeolites and Alumina Based Isomerization Catalysts  
*A. Khodakov, Y. Berthier, J. Oudar, N. Barbouth and P. Schulz* 781
- P075 Characterization of Transition-Metal Ion-Exchanged Zeolites by NMR and EPR Spectroscopy  
*S.-B. Liu, T.C. Yang, R.Y. Lin, E.C. Hong and T.S. Lin* 789
- P076 Photoacoustic Spectroscopy Study of Cobalt Containing Molecular Sieves  
*H.-S. Han and H. Chon* 797
- P077 Electron Spin Echo Modulation Spectroscopic Evidence for Framework Substitution of Ni(I) in NiAPSO-11  
*N. Azuma, C.W. Lee, M. Zamadics and L. Kevan* 805
- P078 Catalytic Properties of VPI-5 Encaged Iron-Phthalocyanines  
*R.F. Parton, C.P. Bezoukhanova, F. Thibault-Starzyk, R. A. Reynders, P. J. Grobet, P. A. Jacobs* 813
- P079 Location and Photostability of faujasite-incorporated methylene-blue  
*R. Hoppe, G. Schulz-Ekloff, D. Wöhrle, Ch. Kirschhock and H. Fuess* 821
- P080 Optical, Electric and Photoelectric Properties of Pure and CdS or CuCl cluster doped Zeolite Single Crystals  
*Yu.A. Barnakov, M.S. Ivanova, V.P. Petranovskii, V.V. Poborchii and V.G. Soloviev* 829
- P081 Magnetic and Optical Properties of Alkali Metal Clusters in LTA  
*Y. Nozue, T. Kodaira, S. Ohwashi, N. Togashi, T. Monji and O. Terasaki* 837
- P082 Polar Arenes in Faujasites  
*C. Kirschhock and H. Fuess* 843

P083	Inelastic Neutron Scattering and Molecular Dynamics Simulations of Water Adsorbed in the Molecular Sieves AlPO <sub>4</sub> -11, AlPO <sub>4</sub> -5, AlPO <sub>4</sub> -8 and VPI-5 <i>F. Trouw, L.E. Iton and M.E. Davis</i>	851
P084	Insight into the Pore Structure of Zeolite MCM-22 through Catalytic Tests <i>A. Corma, C. Corell, A. Martínez and J. Pérez-Pariente</i>	859
P085	Study of Catalytic Properties of SAPO-40 <i>J.P. Lourenço, M.F. Ribeiro, F.R. Ribeiro, J. Rocha, Z. Gabelica, N. Dumont and E. Derouane</i>	867
P087	New Methods for Characterization of External Surface of ZSM-5-Zeolites <i>K.M. Keskinen, T.T. Pakkanen, P. Raulo, M. Ruotsalainen, P. Sarv and M. Tiitta</i>	875
P088	Dielectric Relaxation in Na-MFI Zeolite <i>F. Fernández-Gutierrez, M. Hernández-Velez, H. K. Beyer and R. Roque-Malherbe</i>	883

### Part B.

### III. Modification

A005	Genesis of Rh <sub>n</sub> <sup>0</sup> Clusters in Zeolite Y; Interaction with Zeolite 'Protons' <i>D.C. Tomczak, V.L. Zholobenko, H. Treviño, G-D. Lei and W.M.H. Sachtler</i>	893
A006	Novel Generation of Ionic Clusters within Zeolites <i>Y.S. Park, Y.S. Lee and K.B. Yoon</i>	901
A007	Electronic Modifications in Supported Palladium Catalysts <i>B.L. Mojet, M.J. Kappers, J.C. Muijsers, J.W. Niemantsverdriet, J.T. Miller, F.S. Modica and D.C. Koningsberger</i>	909
A008	Zeolite Encapsulated Metal-Schiff Base Complexes. Synthesis and Electrochemical Characterization <i>F. Bedioui, L. Roue, J. Devynck and K.J. Balkus, Jr.</i>	917
A009	Preparation, Characterization and Catalytic Properties of Cobalt Phthalocyanine Encapsulated in Zeolite EMT <i>S. Ernst, Y. Traa and U. Deeg</i>	925
A023	Solid-State Dealumination of Zeolites <i>H.K. Beyer, G. Borbély-Pálné and J. Wu</i>	933

- C009 The Application of Ru-Exchanged Zeolite NaY in Ammonia Synthesis  
*J. Wellenbüscher, F. Rosowski, U. Klengler, M. Muhler, G. Ertl, U. Guntow and R. Schlögl* 941
- C010 PtCo Bimetallic Particles in NaY Zeolites: Correlation Between Morphology and Reactivity  
*L. Guczi, G. Lu, Z. Zsoldos, Zs. Koppány* 949
- C011 Silver Agglomeration in SAPO-42 and Isostructural Zeolite: EPR and ESEM Studies  
*J. Michalik, M. Zamadics, J. Sadlo and L. Kevan* 957
- C012 Chemistry and Spectroscopy of Chromium in Zeolites  
*B.M. Weckhuysen and R.A. Schoonheydt* 965
- C013 CrAPO-Catalyzed Oxidations of Alkylaromatics and Alcohols with TBHP in the Liquid Phase (Redox Molecular Sieves, Part 8)  
*J.D. Chen, M.J. Haanepen, J.H.C. van Hooff and R.A. Sheldon* 973
- P023 A New Way for Obtaining Acid or Bifunctional Catalysts. Straightforward Calcination of As-Synthesized [Ga]-ZSM-5 Zeolites Obtained from Alkali-Free Media  
*G. Giannetto, R. Monque, R. Galiasso, J. Papa and Z. Gabelica* 981
- P024 Preparation of In- and Ga-Modified SAPO Materials via a Solid State Reaction  
*Ya. Neinska, Ch. Minchev, R. Dimitrova, N. Micheva, V. Minkov and V. Kanazirev* 989
- P025 Determination by IR Spectroscopy of the N(Al<sub>fram</sub>) and Crystallinity Level for Amorphous Phase Containing HY Zeolites  
*O. Cairon, S. Khabtou, E. Balanzat, A. Janin, M. Marzin, A. Chambellan, L.C. Lavalley and T. Chevreau* 997
- P026 Hydrothermal and Alkaline Stability of High-Silica Y-Type Zeolites in Dependence on the Dealumination Procedure  
*W. Lutz, B. Zibrowius and E. Löffler* 1005
- P027 Study on the Nature of Aluminum in Dealuminated Zeolite ZSM-20  
*H. Kosslick, V.A. Tuan, R. Fricke, A. Martin and W. Storek* 1013
- P028 The Effect of Acid Dealumination of Indonesia Zeolite to its Physical, Chemical and Catalytic Properties  
*E. Agustina and T. Pudiyanto* 1021

- P029 Vibrational Spectroscopic Investigations of the Cation Exchange and Thermal Activation of the Silica-Rich Hexagonal Polytype of Faujasitic Zeolites  
*C. Brémard, M. LeMaire, J.M. Manoli and C. Potvin* 1027
- P030 Chemical Vapour Deposition of Si(OEt)<sub>4</sub> on Zeolite H $\beta$   
*Y. Chun, X. Chen, A.Z. Yan, Q.-H. Xu* 1035
- P031 Sensitive Monitoring of Side-Products Formed in Heavy Metal Ion Exchanged Zeolites  
*M. Wark, W. Lutz, E. Löffler, H. Kessler and G. Schulz-Ekloff* 1043
- P032 H- and Cu-Forms of MFI Boralites with Enhanced Number of Skeletal Boron Atoms. Synthesis and Properties  
*L. Kubelková, I. Jirka, J. Vylita, J. Nováková, J. Obsasniková, D. Kolousek* 1051
- P033 Gold Carbonyls and Nitrosyls in Highly Dispersed Au(I) on Zeolite NaY and ZSM-5  
*S. Qiu, W. Pang, W. Xu, R. Xu, R. Ohnishi and M. Ichikawa* 1059
- P034 Stabilization of Silver Clusters in Zeolite Matrices  
*N.E. Bogdanchikova, M.N. Dulin, A.V. Toktarev, G.B. Shevnina, V.N. Kolomiichuk, V.I. Zaikovskii and V. P. Petranovskii* 1067
- P035 Preparation and Testing of Silicalite-in-Metal-Membranes  
*P. Kölsch, D. Venzke, M. Noack, E. Lieske, P. Toussaint and J. Caro* 1075
- P036 MFI-type Zeolite Filled Silicon Rubber Membranes: Preparation, Composition and Performance  
*Y.-C. Long, X. Chen, Z.-H. Ping, S.-K. Fu and Y.-J. Sun* 1083
- P037 Zeolite-Rubber Blend: A Composite with Improved Mechanical and Conducting Properties  
*H. Hamdan, M.N. Mohd Muhid and A. Yahya* 1091
- P038 Preparation and Properties Quantized Semiconductor Particles in Zeolites  
*G. Tel'biz, A. Shwets, V. Gun'ko, J. Stoch, G. Tamulajtis and N. Kukhtarev* 1099
- P039 A New Form of Luminescent Silicon: Synthesis of Silicon Nanocluster in Zeolite Y  
*Ö. Dag, A. Kuperman P.M. Macdonald and G.A. Ozin* 1107
- P040 Synthetic Zeolites as Carrier for Enzyme Immobilization in Laboratory-Scale Fixed-Bed Columns  
*F. Alfani, L. Cantarella, M. Cantarella, A. Gallifuoco and C. Colella* 1115

- P086 Investigation of Surface Reaction Induced Fermi Resonance by IR and MAS NMR Spectroscopy  
*I. Hannus, I.I. Ivanova, G. Tasi, I. Kiricsi and J.B. Nagy* 1123

#### IV. Diffusion and Adsorption

- PL03 Exciting new advances in diffusion of sorbates in zeolites and microporous materials**  
*L. V. C. Rees* 1133
- C001 Simulation of Single Pellet Adsorption Kinetics with Experimentally Determined Dusty-Gas Coefficients  
*R. Hartmann and A. Mersmann* 1151
- C002 Separation of Permanent Gases on the All-Silica 8-Ring Clathrasil DD3R  
*M.J. den Exter, J.C. Jansen and H. van Bekkum* 1159
- C003 Zeolite Filled Membranes for Gas Separation and Pervaporation  
*J.P. Boom, D. Bargeman and H. Strathmann* 1167
- C004 Potentials of Silicalite Membranes for Separation of Alcohol/Water Mixtures  
*T. Sano, M. Hasegawa, Y. Kawakami, Y. Kiyozumi, H. Yanagishita, D. Kitamoto and F. Mizukami* 1175
- C005 Preparation of a Thin Zeolitic Membrane  
*M. Matsukata, N. Nishiyama and K. Ueyama* 1183
- B015 Sorption and Sorption Kinetics of Pyridine in H-ZSM-5 and H-Mordenite  
*W. Niessen and H.G. Karge* 1191
- B016 The Measurement of Diffusion and Adsorption Using a Jetloop Recycle Reactor  
*K.P. Möller, C.T. O'Connor* 1201
- B017 Separation of Cyclohexane from 2,2- and 2,4-Dimethylpentanes by Adsorption in Silicalite  
*C.L. Cavalcante Jr. and D.M. Ruthven* 1209
- B023 DEXAFS Studies on the Diffusion of Ammonia into Zeolite CuNaY-  
*M. Hagelstein, U. Hatje, H. Förster, T. Ressler and W. Metz* 1217
- B024 FTIR Microscopy with Polarized Radiation for the Analysis of Adsorption Processes in Molecular Sieves  
*F. Schüth, D. Demuth and S. Kallus* 1223

- B038 Investigation of Hydrogen and Deuterium Spillover on Y Zeolites by FT-IR Microscopy - Rate Determining Steps  
*U. Roland, R. Salzer and S. Stolle* 1231
- P074 Hydrogen and Deuterium Adsorption on Zeolite Supported Platinum Evidence for Hydrogen and Deuterium Spillover  
*U. Roland, H.G. Karge and H. Winkler* 1239
- P097 Adsorption of Binary Mixture of N<sub>2</sub>, O<sub>2</sub>, and Ar in Zeolite NaCaX  
*N.V. Choudary, R.V. Jasra and S.G.T. Bhat* 1247
- P098 Oxygen Enrichment over Zeolite 5A by a Rapid Pressure Swing Adsorption Process  
*C.-T. Chou and H.-C. Wu* 1255
- P099 A Fourier-Transform Infra-Red Spectroscopic Study of the Adsorption of Hydrogen Cyanide by Zeolites and Pillared Clays  
*J. Jamis, T.D. Smith, T.A.P. Kwack and A. Dyer* 1261
- P100 Experimental and Theoretical Studies of Sulfur Dioxide and Water Adsorption in Hydrophobic Zeolites  
*J. Tantet, M. Eic and R. Desai* 1269
- P101 Dynamic Adsorption Properties of Pelletized Molecular Sieves  
*K. Ehrhardt, A. Seidel-Morgenstern and M. Richter* 1277
- P102 Molecular Sieving of n-Butenes by Zeolite Erionite and by Isostructural Silicoaluminophosphate SAPO-17  
*M. Richter, K. Ehrhardt, U. Roost, H. Kosslick and B. Parltz* 1285
- P103 Separation Properties of H-Mordenite Modified by Anchored Tris(Methyl)-Tin and -Germanium Complexes  
*A. Théolier, A. Choplin, J.M. Basset and E. Benazzi* 1293
- P104 Effect of Size of Solvent Molecule Size on the Adsorption of p- and o-Xylene on ZSM-5 Type Zeolites and Mechanism of Adsorption  
*A. Kurganov, St. Marmé and K. Unger* 1299
- P105 Sorption and Transport of p-Ethyltoluene in H-ZSM-5 Zeolites  
*A. Zikánová, J. Dubsky and M. Kocirik* 1307
- P106 Complex Sorption Rate Behaviour of p-Ethyltoluene, Benzene and n-Hexane on MFI-type Molecular Sieve  
*A. Micke and M. Bülow* 1315

P107	Measurement of Intracrystalline Diffusion by the Zero Length Column Tracer Exchange <i>J.R. Hufton, S. Brandani and D.M. Ruthven</i>	1323
P108	Frequency Response Method for Investigation of Various Dynamic Phenomena Occurring Simultaneously in a Gas/Zeolite System <i>Y. Yasuda</i>	1331
P109	Diffusion of Xylene Isomers in Dealuminated Mazzite Zeolites by the Frequency Response Technique <i>D. McQueen, F. Fajula, R. Dutartre, L.V.C. Rees and P. Schulz</i>	1339
P110	Diffusion of Aromatics Through a Silicalite Membrane <i>D.B. Shah and H.-Y. Lioue</i>	1347
P111	Multicomponent Adsorption Equilibria of Highly Non Ideal Mixtures: The Case of Dimethylnaphthalene Isomers <i>E. Rombi, R. Monaci, I. Ferino, V. Solinas, R. Rota and M. Morbidelli</i>	1355
P112	Adsorption of Glucose and Fructose Containing Disaccharides on Different Faujasites <i>C. Buttersack, W. Wach and K. Buchholz</i>	1363

#### V. Catalysis - First Part

<b>PL04</b>	<b>Catalysis by Zeolites - Science and Technology</b> <i>W. O. Haag</i>	1375
<b>PL07</b>	<b>Zeolites in Environmental Catalysis</b> <i>M. Iwamoto</i>	1395
A015	Adipic Acid Synthesis via Oxidation of Cyclohexene over Zeolite occluded Manganese Diimine Complexes <i>P. P. Knops-Gerits, F. Thibault-Starzyk and P.A. Jacobs</i>	1411
A016	Oxidation of Cyclohexanone and Cyclohexane to Adipic acid by Iron-Phthalocyanine on Zeolite Y <i>F. Thibault-Starzyk, R.F. Parton, P.A. Jacobs</i>	1419
A017	The Effect of Zeolitic Textural Properties on the Catalytic Activity in Hydrocarbons Oxidation <i>F. Cavani, G. Giordano, M. Pedatella and F. Trifirò</i>	1425
A018	Selective Hydrogenation of Cinnamaldehyde Controlled by Host/Guest Interactions in Beta Zeolite <i>P. Gallezot, B. Blanc, D. Barthomeuf and M.-J. Païs da Silva</i>	1433



A019	Benzoylation of Xylenes Using Zeolitic Catalysts <i>R. Fang, H.W. Kouwenhoven and R. Prins</i>	1441
A020	Alkylation of Aniline with Methanol on Beta and EMT Zeolites Exchanged with Alkaline Cations <i>P.R.Hari Prasad Rao, P. Massiani and D. Barthomeuf</i>	1449
A021	Solvent Effects in the Liquid Phase Friedel-Crafts Alkylation over Zeolites: Control of Reaction Rate and Selectivity by Adsorption <i>P.H.J. Espeel, K.A. Verduyze, M. Debaerdemaeker and P.A. Jacobs</i>	1457
A022	<sup>13</sup> C MAS NMR and Related Studies of Coke Formation on H-ZSM-5 <i>H.G. Karge, H. Darmstadt, A. Gutsze, H.-M. Vieth and G. Buntkowsky</i>	1465
B021	Correlation of Adsorption Structure and Reactivity in Zeolite Catalyzed Amination <i>A. Kogelbauer, Ch. Gründling and J.A. Lercher</i>	1475
A035	Structure, Chemistry and Activity of Well-Defined Cu-ZSM-5 Catalysts in the Selective Reduction of NO <sub>x</sub> <i>E.S. Shpiro, R.W. Joyner, W. Grünert, N.W. Hayes, M.R.H. Siddiqui and G.N. Baeva</i>	1483
A036	Copper Ion Exchanged Silicoaluminophosphate (SAPO) as a Thermostable Catalyst for Selective Reduction of NO <sub>x</sub> with Hydrocarbons <i>T. Ishihara, M. Kagawa, F. Hadama and Y. Takita</i>	1493
A037	Active State of Copper in Copper-Containing ZSM-5 Zeolites for Photocatalytic Decomposition of Dinitrogen Monoxide <i>K. Ebitani, M. Morokuma and A. Morikawa</i>	1501
A038	Binding and Catalytic Decomposition of NO by Transition Metal Aluminosilicates <i>K. Klier, R.G. Herman and S. Hou</i>	1507

**Part C.**  
**Catalysis - Second Part**

P065	Decomposition of Sodium Azide in Faujasites of Different Si/Al Ratios <i>M. Brock, C. Edwards, H. Förster and M. Schröder</i>	1515
P113	Contribution of Acidic Properties of Metallosilicate Catalysts to NO Decomposition Reaction <i>S. Iwamoto, S. Shimizu and T. Imui</i>	1523

- P114 The Selective Reduction of NO and Combustion of Paraffins over MFI Zeolites  
*F. Witzel, G. A. Sill and W.K. Hall* 1531
- P115 Catalytic Reduction of Nitric Oxide with Propane over Ln-Pt Ion-Exchanged Zeolites (Ln=Rare Earth)  
*E. Sakamoto, T. Ohnishi and T. Arakawa* 1537
- P116 Alkane Oxidation and N<sub>2</sub>O Decomposition on Cu(II) and Cr (V) Cationic Sites in HZSM-5: Influence of Binding and Poisoning Effect of Sulfate Ions  
*A.V. Kucherov, S.S. Gorjashenko, T.N. Kucherovala, K.I. Slovetskaia and A.A. Slinkin* 1541
- P117 Reaction Mechanism of Selective Reduction of Nitric Oxide by Methane on Ga- and In-ZSM-5 Catalysts  
*K. Yogo and E. Kikuchi* 1547
- P118 Cu Coordination in Zeolitic Matrix. Relationship to Nitric Oxide Binding and Decomposition  
*B. Wichterlová, J. Dedecek and Z. Tvarůzková* 1555
- P119 Reduction Behavior of Copper Oxide in Copper/Mordenites  
*C.Y. Lee and B.H. Ha* 1563
- P120 Zn-Loaded HZSM-5 for Catalytic Reduction of Carbon Dioxide by Propane  
*S. Yamauchi, A. Satsuma, S. Komai, T. Asakawa, T. Hattori and Y. Murakami* 1571
- P121 Zeolites as Catalysts for Decomposition of Sulfur Organic Compounds  
*M. Ziólek and P. Decyk* 1579
- P122 Catalytic Reforming of Methane with Carbon Dioxide over Pentasil Zeolite-Supported Nickel Catalyst  
*J.-S. Chang, S.-E. Park, K.-W. Lee and M.J. Choi* 1587
- P123 Formation of Methyl Formate During Hydrogenation of CO<sub>2</sub> over Cu/ZnO/Al<sub>2</sub>O<sub>3</sub> and K-Fe/L Zeolite Catalysts  
*S.-E. Park, E.K. Shim, K.-W. Lee and P.S. Kim* 1595
- P124 Hydrocarbon Conversions over Sodium Zeolites in the Presence of Hydrogen Sulfide  
*M. Sugioka, M. Amisawa, H. Abe and K. Sato* 1603
- P125 The Effect of Sulfoxide Loadings on the Selectivity and Activity of Zeolite Y for Dehydration Reactions: Stability and Structure of Dithiane Oxide in Zeolite Y  
*S. Feast, D. Bethell, G.J. Hutchings, P.C.B. Page, S.P. Saberi, F. King and C.H. Rochester* 1611

- P126 Zeolite Y Type Supported Nickel and Molybdenum Sulfides. Relation between Metal Sulfide Distribution and Catalytic Properties in Thiophene Hydrodesulfurization  
*G. Vorbeck, W.J.J. Welters, L.J.M. van de Ven, H.W. Zandbergen, J.W. de Haan, V.H.J. de Beer and R.A. van Santen* 1617
- P127 Preparation and Catalytic Behavior of Ternary Oxides of Rhodium or Nickel in the Cages of Zeolite  
*K. Kunimori, M. Seino, D. Nishio and S. Ito* 1625
- P128 Heterogeneous Catalysis of  $\alpha$ -Octene Hydroformylation: The Bimetallic Synergistic Effect for Ru-Co/13X  
*W. Huang, L. Yin and C.-Y. Wang* 1633
- P129 Study of Auto-reduction and Dispersion of Pt in  $\beta$  Zeolite  
*J. Zheng, J.-L. Dong and Q. H. Xu* 1641
- P130 Aromatization of n-Octane over Pt-Based Silicalites: The Influence of Pt Loading and of Added Indium on the Product Distribution in the C<sub>8</sub> Aromatics  
*P. Mériaudeau, G. Sapaly, A. Thangaraj, S. Narayanan and C. Naccache* 1649
- P131 Metal-Resistant FCC Catalysts: Effect of Matrix  
*S.-J. Yang, Y.-W. Chen and C. Li* 1655
- P132 Relationship Between Zeolite Structure and Hydrogen Transfer Reactions in Naphthenes and Paraffins Cracking  
*E. Benazzi, Th. Chapus, T. Cheron, H. Cauffriez and Ch. Marcilly* 1663
- P133 Skeletal Isomerization of n-Butenes on Zeolite Catalysts: Effects of Acidity  
*C.-L. O'Young, W.-Q. Xu, M. Simon and S.L. Suib* 1671
- P134 1-Butene Conversion over SAPO-11 and MeAPO-11  
*S.M. Yang, D.H. Guo, J. S. Lin and G. T. Wang* 1677
- P135 Gas Phase Synthesis of MTBE on Post-Synthesis Modified Zeolites  
*A. Kogelbauer, A.A. Nikolopoulos, J.G. Goodwin, Jr. and G. Marcelin* 1685
- P136 Iso-Butane/1-Butene Alkylation on Zeolites Beta and MCM-22  
*S. Unverricht, S. Ernst and J. Weitkamp* 1693
- P137 Catalytic Properties of Zeolites for Synlube Production by Olefins Oligomerization  
*P.-S.E. Dai, J.R. Sanderson and J.F. Knifton* 1701

- P138 Propene Oligomerization and Xylene and Methyl-Pentene Isomerization over SAPO-11 and MeAPSO-11  
*J.S. Vaughan, C.T. O'Connor and J.C.Q. Fletcher* 1709
- P139 Temperature switched in situ  $^1\text{H}$  and  $^{13}\text{C}$  MAS NMR Studies of the Catalytic Conversion of Methanol on Zeolite ZSM-5  
*H. Ernst, D. Freude, T. Mildner and H. Pfeifer* 1717
- P140 Effect of the Binder on the Properties of a Mordenite Catalyst for the Selective Conversion of Methanol into Light Olefins  
*J.M. Fougerit, N.S. Gnep, M. Guisnet, P. Amigues, J. L. Duplan and F. Hugues* 1723
- P141 Understanding the Brønstedt Acidity of SAPO-5, SAPO-17, SAPO-18 and SAPO-34 and their Catalytic Performance for Methanol Conversion to Hydrocarbons  
*J. Chen, P.A. Wright, S. Natarajan and J.M. Thomas* 1731
- P142 Formation of Methane from the Conversion of Methanol and Propene over ZSM-5 at Temperatures above 450°C  
*M.G. Howden, W.P. Müller* 1739
- P143 Reactivation of Coked HZSM-5 by Hydrogen and by Alkane Treatment  
*F. Bauer, E. Geidel and E. Petzold* 1749
- P144 Interaction of  $\text{C}_2\text{-C}_6$ -Hydrocarbons with Surfaces of H-ZSM-5 and Ga-H-ZSM-5 Zeolites  
*O.P. Keipert and M. Baerns* 1757
- P145 Aromatization of n-Pentane over Ni-ZSM-5 Catalysts  
*S.-K. Ihm, K.-H. Yi and Y.-K. Park* 1765
- P146 Ag-ZSM-5 as a Catalyst for Aromatization of Alkanes, Alkenes, and Methanol  
*Y. Ono, K. Osako, G.-J. Kim and Y. Inoue* 1773
- P147 BTX Aromatics from the Hydroconversion of Heavy Alkylate over Alumina-Deficient Mordenite Catalysts  
*R.M. Habib, F.I. Kenawi, A.K. El-Morsi and R.A. El-Adly* 1781
- P148 The Catalyst Deactivation in Alkylation of Xylenes with Methanol Using Type Y Zeolite  
*M.E. Pitkänen and A.O.I. Krause* 1789
- P149 Benzene Alkylation over Ga, B and Al Pentasils  
*A.V. Smirnov, B.V. Romanovsky, I.I. Ivanova, E.G. Derouane and Z. Gabelica* 1797

- P150 Ethylbenzene Disproportionation over Large Pore Zeolites  
*H.G. Karge, S. Ernst, M. Weihe, U. Weiß and J. Weitkamp* 1805
- P151 Hydrodimerization of Benzene and Alkylbenzene over Polyfunctional Zeolite Catalysts  
*V.I. Smirnitsky, V.A. Plakhotnik, I.I. Lishchiner and E.S. Mortikov* 1813
- P152 Selective Formation of 2,6-Dimethylnaphthalene from 2-Methylnaphthalene on ZSM-5 and Metallosilicates with MFI Structure  
*T. Komatsu, Y. Araki and S. Namba and T. Yashimae* 1821
- P153 Methylation, Isomerization and Disproportionation of Naphtalene and Methylnaphthalenes on Zeolite Catalysts  
*Z. Popova, M. Yankov and L. Dimitrov* 1829
- P154 The Isopropylation of Naphthalene over Cerium-Modified H-Mordenite  
*Y. Sugi, J.-H. Kim, T. Matsuzaki, T. Hanaoka, Y. Kubota, X. Tu and M. Matsumoto* 1837
- P155 Alkylation of Binuclear Aromatics with Zeolite Catalysts  
*A.S. Loktev and P.S. Chekriy* 1845
- P156 Ti Substituted Zeolite Beta (Ti- $\beta$ ) Catalyzed Selective Epoxidation of 1-Octene with Hydrogen Peroxide  
*T. Sato, J. Dakka and R.A. Sheldon* 1853
- P157 Factors Determining Substrate Specificity in Titanium Silicalite Catalyzed Oxidations  
*T. Tatsumi, K. Asano and K. Yanagisawa* 1861
- P158 Oxidation of Saturated Hydrocarbons Involving CoAPO Molecular Sieves as Oxidants and as Catalysts  
*B. Kraushaar-Czarnetzki, W.G.M. Hoogervorst and W.H.J. Stork* 1869
- P159 Cyclohexane Oxidation with Hydrogen Peroxide Catalyzed by Titanium Silicalite (TS-1)  
*U. Schuchardt, H.O. Pastore and E.V. Spinacé* 1877
- P160 Chemoselective Oxidation of Organic Compounds Having Two or More Functional Groups  
*A. Bhaumik, R. Kumar and P. Ratnasamy* 1883
- P161 Cyclohexanol and Cyclohexanone Reactions on HZSM-5 Zeolites  
*L. Brabec, J. Nováková and L. Kubelková* 1889
- P162 Beckmann Rearrangement of Cyclohexanone Oxime on the External Surface of Zeolite Crystals  
*T. Yashima, K. Miura and T. Komatsu* 1897

- P163 Anthraquinones Formation on Zeolites with BEA Structure  
*O.V. Kikhtyanin, K.G. Ione, G.P. Snytnikova, L.V. Malysheva, A.V. Toktarev, E.A. Paukshtis, R. Spichtinger, F. Schüth and K. K. Unger* 1905
- P164 Aldol Condensation of Acetone over Alkali Cation Exchanged Zeolites  
*C.O. Veloso, J.L.F. Monteiro and E.F. Sousa-Aguiar* 1913
- P165 Methyl  $\alpha$ -Hydroxyisobutyrate Dehydration over Zeolite Catalysts  
*K.J. Balkus, Jr., A.K. Khanmamedova and S. Kowalak* 1921
- P166 Studies on the Nature of Catalysts for the Selective Synthesis of Methylamine  
*Y.-Z. Zhang, Z.-L. Xu, J. Wang and Y.-Y. Ke* 1927
- P167 Activity of Ga, In and Cu Modified MFI Zeolites for Amine Reactions  
*V. Kanazirev and G.L. Price* 1935
- P168 Selective Synthesis of Ethylenediamine from Ethanolamine over Zeolite Catalysts  
*K. Segawa, S. Mizuno, Y. Maruyama and S. Nakata* 1943
- P169 Vapor Phase Synthesis of Pyridine Bases From Aldehydes And Ammonia Over Pentasil Zeolites  
*H. Sato, S. Shimizu, N. Abe and K.-I. Hirose* 1951
- P170 Methylation of Pyridine over Zeolites  
*U. Kameswari, C.S. Swamy and C.N. Pillaie* 1959
- P171 Synthesis of Substituted Pyrroles by Heterogeneous-Catalytic Conversion of 2-Methylfuran and Amines on Zeolite Catalysts  
*A. Martin and B. Lücke* 1965
- P172 Vapour-Phase Nitration of Benzene over Zeolitic Catalysts  
*L. Berteau, H.W. Kouwenhoven and R. Prins* 1973
- P173 Substitution of Halobenzenes to Aniline or Phenol, Catalyzed by Copper-Exchanged Zeolites. Selectivity Improvements and Reaction Pathway  
*M.H.W. Burgers and H. van Bekkum* 1981
- P174 Reaction of p-Dihalobenzenes over Zeolites  
*T. Takahashi and T. Kai* 1989
- P175 Selective Synthesis of Isoprene by Prins Condensation Using Molecular Sieves  
*E. Dumitriu, V. Hulea, C. Chelaru, T. Hulea and S. Kaliaguine* 1997

- P176 Use of Very Large Pore Molecular Sieves for the Gas-Phase Synthesis of 2,4-Diphenyl-4-Methylpentenes  
*J. Issakov, E. Litvin, Ch. Minachev, G. Öhlmann, V. Scharf, R. Thome, A. Tiffler and B. Unger* 2005
- P177 MCM-41 and Related Materials as Media for Controlled Polymerization Processes  
*P.L. Llewellyn, U. Ciesla, H. Decher, R. Stadler, F. Schüth and K.K. Unger* 2013
- P178 Pt-Containing Zeolites for Enantioselective Catalytic Hydrogenation of Ethyl-Pyruvate - Effects of Zeolite Structures, Solvent and Modifier Concentration  
*W. Reschetilowski, U. Böhmer and J. Wiehl* 2021
- P179 Application of Microporous Materials for Catalytic Disproportionation of Alkylsilanes  
*F. Bouchet, H. Fujisawa, M. Kato and T. Yamaguchi* 2029

## VI. Theory and Modelling

- PL05 Structure and Reactivity of Zeolite Catalysts: Atomistic Modelling using ab initio Techniques**  
*J. Sauer* 2039
- C006 Computer Simulations Benzene in Faujasite-Type Zeolites  
*N.J. Henson, A.K. Cheetham, A. Redondo, S.M. Levine and J.M. Newsam* 2059
- C007 Aromatic Molecules in Zeolite Y. A Model System for Catalytic Processes?  
*H. Klein and H. Fuess* 2067
- C008 Computer Modelling of Sorbates and Templates in Microporous Materials  
*R.G. Bell, D.W. Lewis, P. Voigt, C.M. Freeman, J.M. Thomas and C.R.A. Catlow* 2075
- C014 Interatomic Potentials for Zeolites - Derivation of an Ab-Initio Shell Model Potential  
*K. de Boer, A.P.J. Jansen and R.A. van Santen* 2083
- C015 Vibrational Structure of Zeolite A  
*M. Bärtsch, P. Bornhauser, G. Calzaferri and R. Imhof* 2089
- C016 Low-Occupancy Sorption Thermodynamics of Long Alkanes in Silicalite via Molecular Simulation  
*E.J. Maginn, A.T. Bell and D.N. Theodorou* 2099

- C017 Molecular Dynamics Simulations of Diffusion in a Cubic Symmetry Zeolite  
*P. Demontis and G.B. Suffritti* 2107
- C018 Molecular Modelling Studies of Zeolite Synthesis  
*P.A. Cox, A.P. Stevens, L. Banting, E. M. Gorman* 2115
- C019 Ti Substitution in MFI Type Zeolites: A Quantum Mechanical Study  
*R. Millini, G. Perego and K. Seiti* 2123
- P089 Molecular-Dynamical Calculations of the Vibrational Spectra of Hydrocarbons Adsorbed in Silicalite and Zeolite A  
*D. Dumont and D. Bougeard* 2131
- P090 An MD Study of Methane Diffusion in Zeolites of Structure Type LTA  
*S. Fritzsche, R. Haberlandt, J. Kärger, H. Pfeifer and M. Waldherr-Teschner* 2139
- P091 Vibrational Frequency Shift Calculation of Diatomic Molecules in A-Type Zeolite  
*A.V. Larin, F. Jousse and E. Cohen De Lara* 2147
- P092 Pt-Mordenite Catalyst: A Molecular Graphics Study  
*F. Blanco, G. Urbina-Villalba and M.M. Ramirez de Agudelo* 2155
- P093 Theoretical Methods for Estimating Brønsted Acid Site Strength in Zeolites: Application to Isomorphously Substituted Systems  
*P.J. O'Malley* 2163
- P094 Quantum-Chemistry Calculations of Surface Complex and Orbital Control in Para/Ortho Toluene Alkylation Catalyzed by Big Pore Zeolites  
*A. Corma, G. Sastre and P. Viruela* 2171
- P095 The IR Transmission Windows of Hydrogen Bonded Complexes in Zeolites: A New Interpretation of IR Data of Acetonitrile and Water Adsorption on Zeolitic Brønsted Sites  
*A.G. Pelmenschikov, R.A. van Santen, J.H.M.C. van Wolput and J. Jänchen* 2179
- P096 Heterogeneity of Hydroxyl Groups in Faujasites of Various Si/Al: IR and NMR Studies, Quantum Chemical MNDO Calculations  
*J. Datka, E. Broclawik, J. Klinowski and B. Gil* 2187



## VII. Industrial Applications and Novel Materials

<b>PL06</b>	<b>Industrial Applications of Zeolite Catalysis</b>	
	<i>J. E. Naber, K. P. de Jong, W. H. J. Stork, H. P. C. E. Kuipers and M. F. M. Post</i>	2197
B005	Nitrido Zeolites - a Novel and Promising Class of Compounds	
	<i>W. Schnick</i>	2221
B006	The Synthesis and Structure of a New Open Framework Zinc Phosphate. $Zn_2P_2O_8C_2N_2H_{10}$	
	<i>R.H. Jones, J. Chen, G. Sankar and J.M. Thomas</i>	2229
B007	Novel Molecular Sieves of the Aluminophosphate Family: $AlPO_4$ and Substituted Derivates with LTA, FAU and AFR Structure-Types	
	<i>L. Sierra, J. Patarin, C. Deroche, H. Gies and J.L. Guth</i>	2237
B008	Titanium-Containing Large Pore Molecular Sieves from Boron-Beta: Preparation, Characterization and Catalysis	
	<i>M.S. Rigutto, R. de Ruiter, J.P.M. Niederer and H. van Bekkum</i>	2245
B009	Synthesis and Characterization of a Novel Microporous Indiumphosphate	
	<i>Y. Xu, L.L. Koh, L.H. An, S.-L. Qiu and Y. Yue</i>	2253
B025	Comparative Spectroscopic Study of TS-1 and Zeolite-Hosted Extraframework Titanium Oxide Dispersions	
	<i>J. Klaas, K. Kulawik, G. Schulz-Ekloff and N.I. Jaeger</i>	2261
B026	Conducting Polymer Wires in Mesopore Hosts	
	<i>C.-G. Wu, T. Bein</i>	2269
B027	Optical Properties of Self-Assembled Dipole Chains in Zeolites	
	<i>F. Marlow, K. Hoffmann, W. Hill, J. Kornatowski and J. Caro</i>	2277
B028	Polarized Absorption and Raman Spectra of 1-Dimensional Selenium Chains in Mordenite and Cancrinite Single Crystals	
	<i>V.V. Poborchii, M.S. Ivanova and S.S. Ruvimov</i>	2285
B029	Positron Annihilation in $Cd^{2+}$ Ion-Exchanged and CdS Loaded Zeolite Y	
	<i>Y.-J. He and Y. Hu</i>	2295
A030	Examination of the 'Decomposition Behaviour' of Zeolite A in Freshwater, Particularly Taking into Consideration Environmentally Relevant Conditions	
	<i>P. Kuhm and W. Lortz</i>	2303

A031	Zeolite Catalysis for Upgrading Gasoline <i>C.Y. Yeh, H.E. Barner and G.D. Suci</i>	2311
A032	Studies on Wax Isomerization for Lubes and Fuels <i>S.J. Miller</i>	2319
A033	Skeletal Isomerisation of Olefins with the Zeolite Ferrierite as Catalyst <i>H.H. Mooiweer, K.P. de Jong, B. Kraushaar-Czarnetzki, W.H.J. Stork and B.C.H. Krutzen</i>	2327
A034	Effect of Temperature on Propane Aromatization by Ga/H MFI (Si, Al) Catalysts <i>S. B. Abdul Hamid, E.G. Derouane, P. Mériaudeau, C. Naccache and M. Ambar Yarmo</i>	2335
	<b>Author Index</b>	2345
	<b>Subject Index</b>	2355

## Conducting Polymer Wires in Mesopore Hosts

C.-G. Wu and T. Bein\*

Department of Chemistry, Purdue University, West Lafayette, IN 47907, USA.

Nanometer-size conducting structures are of great interest in view of fundamental issues and potential applications. We explore the inclusion chemistry of conjugated polymers and graphite-like materials as a means to create such structures. Novel mesoporous materials with pore diameters in the 3 nm range (MCM-41) are used as hosts. Monomer molecules are introduced *via* vapor or solution transfer and polymerized either by included or external reagents. The properties of the conjugated systems are studied while encapsulated or after dissolution of the host. In the case of polyaniline formed on oxidation of aniline with persulfate, microwave absorption shows the presence of *conducting filaments* in the host channels. The above systems are compared with graphite-type material encapsulated in MCM-41 by first forming a precursor polymer such as polyacrylonitrile that is pyrolyzed at 500-800°C. These polymer chains are the first nanometer-size conducting filaments stabilized in a well-defined channel host.

### 1. INTRODUCTION

Intensive efforts are directed at the reduction of the size of electronic components, in order to increase storage capacity and speed in information processing. At the culmination of this development one could envisage devices with components of *molecular size*.<sup>1</sup> While still mostly at the conceptual stage, "molecular electronics" has inspired much interesting research directed at building devices from molecular assemblies. Organic conducting polymers<sup>2</sup> with their characteristic quasi one-dimensional chain structure and good conductivity might offer the best potential to control charge transport at molecular dimensions.

We have demonstrated the preparation of nanometer-size polymer filaments such as polypyrrole, polyaniline, polythiophene, and pyrolyzed polyacrylonitrile in zeolites with channels smaller than about one nanometer.<sup>3</sup> Precursor monomers are introduced into the zeolite host and are subsequently polymerized by appropriate oxidants in the pore system. Using microwave absorption measurements, it was found that *charged* polymers encapsulated in these narrow pores are not conducting, apparently because the charge carriers are trapped by the channel walls.<sup>4</sup>

Encapsulation of conducting polymer filaments in various host structures has recently been developed. For example, polypyrrole and polythiophene fibers of about 0.1-1  $\mu\text{m}$  in width have been grown electrochemically within microporous membranes, such as Anopore alumina filtration membranes<sup>5</sup>. Methylacetylene gas reacts with the acid sites in various zeolites to form conjugated oligomers,<sup>6</sup> and polyacetylene was formed in different forms of mordenite.<sup>7</sup>

We have now extended our studies of polyaniline and pyrolyzed polyacrylonitrile to the newly developed mesoporous aluminosilicate hosts, MCM-41, which offer much larger channel diameters than classical zeolites.<sup>8</sup>

## 2. EXPERIMENTAL

The MCM-41 host was synthesized with  $\text{C}_{16}\text{H}_{33}\text{N}(\text{CH}_3)_3\text{OH}$  according to ref. 8, with a Si/Al ratio of 18, and calcined at 580 °C. Before loading with monomers, the hosts used in this study were pretreated with oxygen and vacuum at high temperature (12 h at 400°C,  $10^{-5}$  torr) to remove water and trace amounts of absorbed organic molecules. To load with copper ions, 1.00 g of the calcined MCM was stirred for 3 h at 25 °C with 100 mL of 0.1 M Cu(II)nitrate (aq), filtered, and washed with water. These steps were repeated four times. Slight decreases in crystallinity were observed.

Polyaniline was formed by adsorbing dried and vacuum-distilled aniline into the host from the vapor phase at 40 °C for 24 h; a maximum of 0.3 g aniline adsorbed in 1.0 g of CuMCM host (Sample AN-CuMCM). The saturated host was then immersed in an aqueous solution of peroxodisulfate at 0 °C for 4 h (mole ratio of oxidant vs. aniline 1:1, 1 g of AN-CuMCM in 50 ml 0.2 M HCl) and a drastic color change to dark green was observed. After thorough washing with water, the materials were dried under vacuum (Sample PANI-CuMCM). A typical polymer loading is 0.16 g per 1.00 g of CuMCM host.

Polyacrylonitrile was introduced as follows. MCM-41 was contacted with degassed (three cycles of freeze-pump-thaw) acrylonitrile vapor at room temperature for 4 hours. The acrylonitrile loaded MCM-41 (ANZ) was evacuated to remove the molecules absorbed on the surface of the host. Under nitrogen, ANZ was mixed with distilled H<sub>2</sub>O (typically 1.00 g of ANZ with 20 ml of water). The temperature was raised to 40°C, then K<sub>2</sub>S<sub>2</sub>O<sub>8</sub>(aq) and NaHSO<sub>3</sub>(aq) were added. The mixture was stirred at 40°C under nitrogen for 20 hours; the solids were filtered off, washed with water and dried under vacuum. The resulting white solid (PANZ) was pyrolyzed under nitrogen at different temperatures between 500°C and 800°C for 24 hours (PPANZ).

### 3. RESULTS AND DISCUSSION

#### 3.1. Polyaniline in mesoporous hosts

The conductivity of polyaniline is not only controlled by the degree of chain oxidation, but also by the level of protonation in  $\{[(-B-NH-B-NH-)_{y}(-B-N=Q=N-)_{1-y}] (HA)_{x}\}_{n}$ .<sup>9</sup> In the emeraldine salt (PANI),  $y$  is close to 0.5; B, Q are C<sub>6</sub>H<sub>4</sub> rings in the benzenoid and quinoid states, and HA is an acid.

Here we will discuss a representative preparation, using a copper-exchanged MCM host that was equilibrated with aniline and contacted with peroxydisulfate. The copper ion content in CuMCM is rather low (0.21 Cu/Al). Therefore there may not be sufficient oxidant to polymerize large amounts of polyaniline inside the host. By carrying out the reaction in air, oxygen could be the indirect oxidant which continues to oxidize the Cu<sup>+1</sup> to Cu<sup>+2</sup> during the reaction. However, we find that such conditions will produce non-conducting leucoemeraldine or mixtures of products, but not the conducting emeraldine salt.

When the exposure to aniline vapor is carried out under vacuum, no polymer is formed (sample AN-CuMCM). The pink products may contain some radicals and cations of aniline or its oligomers, as indicated by an electronic absorption peak at 410 nm, suggesting the presence of nitrenium cations (C<sub>6</sub>H<sub>5</sub>NH<sup>+</sup>) or nitrenium radicals (C<sub>6</sub>H<sub>5</sub>NH·).<sup>10</sup> The cations and radicals are quite reactive; upon contact with air, the color turns brown.

If the pink material is reacted with (NH<sub>4</sub>)<sub>2</sub>S<sub>2</sub>O<sub>8</sub>/HCl aqueous solution under exclusion of air, the resulting dark green product, PANI-CuMCM, contains the *emeraldine salt form* (diagnostic IR peaks at 1581, 1497, 1300, and 1230 cm<sup>-1</sup>).<sup>11</sup> The electronic absorption spectrum of PANI-CuMCM shows peaks at 3.4 and 1.6 eV, typical for the band-gap and polaron transitions of emeraldine salt.<sup>12</sup> The encapsulated, evacuated

polymer exhibits a single fairly broad (8 G) ESR line at  $g=2.0057$ . The rather large linewidth could suggest slightly lower protonation levels than in emeraldine salt,<sup>13</sup> or dipolar interactions with the MCM channel walls.

Thermogravimetric experiments in oxygen show that the stability of PANI-CuMCM is higher (decomposition between 350-600 °C) than that of bulk PANI (rapid decomposition between 300-400 °C) (Figure 1). This indicates hindered diffusion of reactants and products during the pyrolysis reactions. In contrast, with AN-CuMCM the major weight loss occurs below 200 °C.

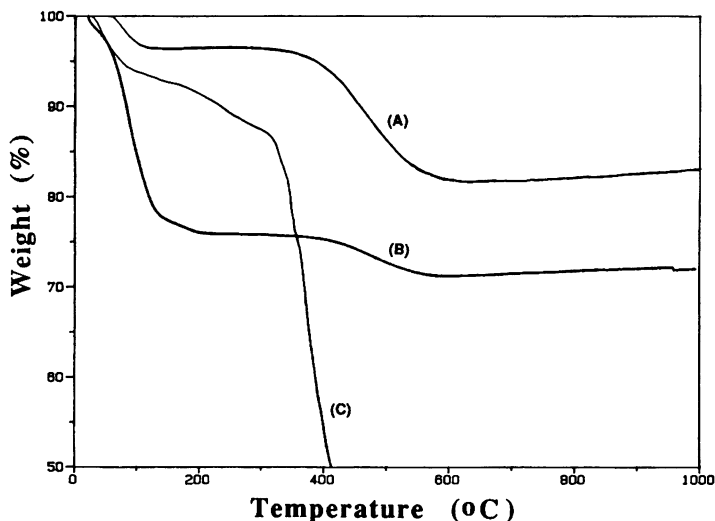


Figure 1. Thermogravimetric analysis in oxygen of (A) PANI-CuMCM, (B) AN-CuMCM, and (C) bulk PANI. Heating rate: 5 °C/min with 100 mL/min oxygen.

The location of the polymer (inside vs. outside of the channels) is an important aspect of these systems. Infrared spectra of the hydroxyl region of CuMCM before aniline loading show a single peak at  $3691\text{ cm}^{-1}$  (in Nujol), which disappears on contact with aniline. This indicates complete coverage of the intrachannel surface with aniline. The intrachannel volume reduction after polymerization was probed with

nitrogen sorption. The nitrogen sorption isotherm of PANI-CuMCM shows a residual pore volume of 0.43 ml per g of CuMCM host, compared with 0.64 ml pore volume in the empty host. If a polymer density of unity is assumed, the loading of 0.16 g/(g host) is close to the expected change in porosity probed with nitrogen sorption. Even after loading with polymer, the tubular structure of the channels is maintained as indicated by a similar isotherm shape. The shift of the saturation transition to lower partial pressure shows that the channels are now narrowed.

What is the conductivity of the encapsulated PANI? Transport studies of bulk emeraldine salt have led to the model of a granular metal where charge hopping in amorphous regions between metallic bundles dominates the macroscopic conductivity.<sup>14</sup> The d.c. conductivity of a compressed pellet of PANI-CuMCM is in the range of  $10^{-8}$  S/cm. This is not more than the conductivity of unloaded CuMCM, and many orders of magnitude lower than bulk PANI, demonstrating that no significant conducting paths develop on the crystal surfaces. The microwave cavity perturbation technique<sup>15</sup> was used to probe the charge transport of PANI filaments in the MCM host. The microwave conductivity (at 2.63 GHz) of dry PANI-CuMCM is *only 10 times less than that of as-synthesized bulk PANI* (d.c. conductivity of 0.2 S/cm), after correction for the volume fraction of the polymer in the host. This significant conductivity is striking evidence that conjugated polymers can be encapsulated in nanometer channels and still support mobile charge carriers. The channels of the CuMCM host provide enough space for important polyaniline interchain contacts.

### 3.2. Pyrolyzed polyacrylonitrile in mesoporous hosts

Pyrolyzed polyacrylonitrile (PAN) was chosen as an alternative example for intrachannel conducting materials. Polymerization of acrylonitrile proceeds in the presence of free radical or anionic initiators, and pyrolysis produces a ladder polymer by cyclization through the nitrile pendant group. At higher temperature, a graphite-like structure with increased conductivity is formed, in which the delocalized electrons contribute to the charge transport.<sup>16</sup> The polymerization of acrylonitrile in montmorillonite<sup>17</sup> has been reported, but these systems contain sheets of micrometer dimensions, different from the nanometer channels of the MCM hosts.

The vapor transfer of acrylonitrile into the host can be easily achieved at room temperature. The terminal hydroxyl groups of MCM-41 are still observed after inserting acrylonitrile, but at the same time a significant peak at  $2244\text{ cm}^{-1}$ , which is the characteristic vibration of

CN, appears. The acid-base interaction between guest and host observed in the above aniline/CuMCM-41 system was not detected here, due to the weaker basicity of acrylonitrile compared to aniline. X-ray diffraction data show that the crystallinity of the host is intact after insertion of polyacrylonitrile, and even after pyrolysis at 800°C.

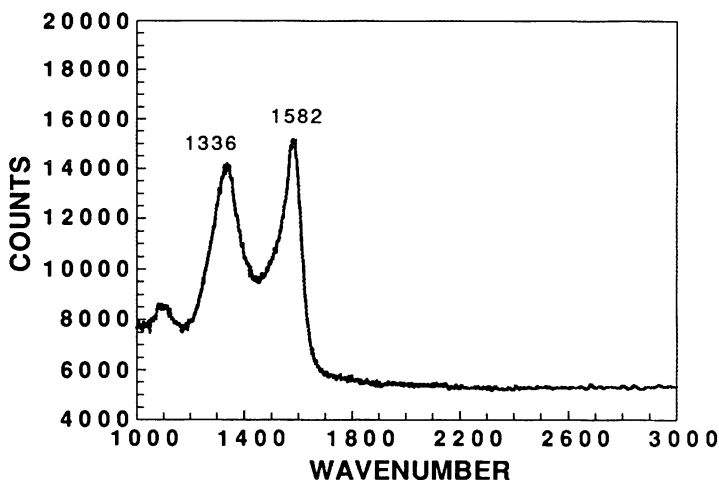


Figure 2. Raman spectrum of sample PPAZ (800 °C, 24 h). Excitation with ca. 50 mW at 514.5 nm.

The IR spectrum of polyacrylonitrile pyrolyzed at 800°C is featureless, however the Raman spectrum shows two distinct peaks at relative wavenumbers of 1582  $\text{cm}^{-1}$  and 1336  $\text{cm}^{-1}$  which are similar to the characteristic vibrations of graphite<sup>16</sup> (Figure 2). The diffuse reflectance UV spectrum of pyrolyzed polyacrylonitrile/MCM between 200 and 800 nm is also similar to that of graphite.

The nitrogen content of pyrolyzed polyacrylonitrile not only depends on the pyrolysis temperature but also on the polymer environment. In general, for the same pyrolysis temperature, polyacrylonitrile in MCM-41 has a higher C/N ratio compared to bulk polymer (Table 1).

The normalized microwave conductivity of PPAZ (with ca.12 wt% of  $\text{CH}_x$ ) is higher than that of the bulk polymer. This is consistent with the formation of graphite-like material in the polyacrylonitrile/MCM system. The microwave conductivity also increases with the pyrolysis temperature as shown in Table 1. Furthermore, the formation of



graphite-like material *inside* the channels of the MCM-41 host is supported by the volume decrease observed in nitrogen sorption isotherms.

In conclusion, we have achieved the fabrication of 'molecular wires' based on conducting polymers in nanometer channels. This type of stabilized conducting systems will be important for the development and understanding of nanometer-size electronic devices.

Table 1.

The C/N ratio and AC conductivity at 2.63 GHz of bulk polyacrylonitrile and polyacrylonitrile/MCM pyrolyzed at different temperatures.

Sample	Pyrolysis conditions	C/N ratio	AC conductivity (S/cm) <sup>a</sup>
Polymer/MCM	800°C 24 hr.	9.86	$1.4 \times 10^{-1}$
Bulk polymer	800°C 24 hr.	8.87	$4.8 \times 10^{-3}$
Polymer/MCM	650°C 24 hr.	5.15	$1.7 \times 10^{-2}$
Bulk polymer	650°C 24 hr.	4.50	$4.4 \times 10^{-3}$
Polymer/MCM	500°C 24 hr.	3.92	$2.0 \times 10^{-3}$
Bulk polymer	500°C 24 hr.	3.79	$1.2 \times 10^{-3}$

<sup>a</sup>The density of pyrolyzed polyacrylonitrile was assumed to be 2.0 g/cm<sup>3</sup>.

#### 4. ACKNOWLEDGMENT

The authors thank Sprague Electric Co. for partial funding of this work. We appreciate the contribution of Stephane Esnouf to the microwave measurements.

## 5. REFERENCES

- 1 Molecular Electronic Devices II; F. L. Carter, Ed., Marcel Dekker, New York, 1987.
- 2 Handbook of Conducting Polymers; T. A. Skotheim, Ed.; Marcel Dekker, New York, Vol. 1, 1986.
- 3 (a) P. Enzel and T. Bein, *J. Phys. Chem.*, 93 (1989) 6270.  
(b) P. Enzel and T. Bein, *J. C. S., Chem. Commun.* (1989) 1326.  
(c) T. Bein and P. Enzel, *Angew. Chem. Int. Ed. Engl.*, 28 (1989) 1692.  
(d) T. Bein and P. Enzel, *Mol. Cryst. Liq. Cryst.*, 181 (1990) 315.  
(e) P. Enzel, J. J. Zoller and T. Bein, *J. C. S., Chem. Commun.* (1992) 633.  
(f) P. Enzel and T. Bein, *Chem. Mater.*, 4 (1992) 819.
- 4 L. Zuppiroli, F. Beuneu, J. Mory, P. Enzel and T. Bein, *Synth. Met.*, 55 (1993) 5081.
- 5 Z. Cai and C. R. Martin, *J. Am. Chem. Soc.*, 111 (1989) 4138.
- 6 S. D. Cox and G. D. Stucky, *J. Phys. Chem.*, 95 (1991) 710.
- 7 G. J. Millar, A. R. Lewis, G. A. Bowmaker and R. P. Cooney, *J. Mater. Chem.*, 3 (1993) 867.
- 8 (a) J. S. Beck, U. S. Patent 5,057,296, Oct. 15, 1991.  
(b) J. S. Beck et al., *J. Am. Chem. Soc.*, 114 (1992) 10834.
- 9 A. G. MacDiarmid and A. J. Epstein, *Faraday Discuss. Chem. Soc.*, 88 (1989) 317.
- 10 M. Lapkowski, *Synth. Met.*, 35 (1990) 169.
- 11 Y. Furukawa, F. Ueda, Y. Hyodo, I. Harada, T. Nakajima and T. Kawagoe, *Macromolecules*, 21 (1988) 1297.
- 12 L. W. Shacklette, J. F. Wolf, S. Gould and R. H. Baughman, *J. Chem. Phys.*, 88 (1988) 3955.
- 13 H. H. S. Javadi, R. Laversanne, A. J. Epstein, R. K. Kohli, E. M. Scherr and A. G. MacDiarmid, *Synth. Met.*, 29 (1989) E439.
- 14 Z. H. Wang, E. M. Scherr, A. G. MacDiarmid and A. J. Epstein, *Phys. Rev. B*, 45 (1992) 4190.
- 15 D. C. Dube, M. T. Lanagan, J. H. Kim and S. J. Jang, *J. Appl. Phys.*, 63 (1988) 2466.
- 16 C. L. Renschler, A. P. Sylwester and L. V. Salgado, *J. Mat. Res.*, 4 (1989) 452.
- 17 N. Sonobe, T. Kyotani, Y. Hishiyama, M. Shiraishi and A. Tomita, *J. Phys. Chem.*, 92 (1988) 7029.